



Research
Bridge Engineering—Article

Damping Identification of Bridges Under Nonstationary Ambient Vibration

Sunjoong Kim, Ho-Kyung Kim*

Department of Civil and Environmental Engineering, Seoul National University, Seoul 08826, Korea

ARTICLE INFO

Article history:

Received 18 April 2017
Revised 27 August 2017
Accepted 22 November 2017
Available online 23 November 2017

Keywords:

Damping
Operational modal analysis
Traffic-induced vibration
Nonstationary
Signal stationarization
Amplitude-modulating
Bridge
Cable-stayed
Suspension

ABSTRACT

This research focuses on identifying the damping ratio of bridges using nonstationary ambient vibration data. The damping ratios of bridges in service have generally been identified using operational modal analysis (OMA) based on a stationary white noise assumption for input signals. However, most bridges are generally subjected to nonstationary excitations while in service, and this violation of the basic assumption can lead to uncertainties in damping identification. To deal with nonstationarity, an amplitude-modulating function was calculated from measured responses to eliminate global trends caused by nonstationary input. A natural excitation technique (NEXt)-eigensystem realization algorithm (ERA) was applied to estimate the damping ratio for a stationarized process. To improve the accuracy of OMA-based damping estimates, a comparative analysis was performed between an extracted stationary process and nonstationary data to assess the effect of eliminating nonstationarity. The mean value and standard deviation of the damping ratio for the first vertical mode decreased after signal stationarization.

© 2017 THE AUTHORS. Published by Elsevier LTD on behalf of Chinese Academy of Engineering and Higher Education Press Limited Company. This is an open access article under the CC BY-NC-ND license (<http://creativecommons.org/licenses/by-nc-nd/4.0/>).

1. Introduction

The damping ratio is known to have a strong correlation with the occurrence of vortex-induced vibration in long-span bridges [1,2]. To estimate the damping ratios of long-span bridges, many researchers have utilized output-only operational modal analysis (OMA), instead of using heavy exciters that would require the temporary closure of bridges in use. One of the important assumptions of output-only OMA is that a structural system should be under stationary ambient vibration. However, nonstationary loads such as earthquakes, extreme winds, and traffic are the main sources of excitation in civil infrastructures, and these loads cause nonstationary responses [3–5]. Thus, the violation of excitation conditions for the basic assumption of a classic OMA could be one of the reasons for poor estimation of damping ratios.

Traffic loads are the main loading source for bridges [6,7], and can be expressed as a stationary random process since the roughness of a road is modeled as a zero-mean stationary Gaussian random process [8]. However, when traffic volume is low, an ambient vibration signal at the sensor position is seen as an envelope as a

vehicle approaches and fades away. The traffic-induced vibration (TIV) observed at a specific position can be read as a nonstationary process that is expressed as a product of stationary white noise and an envelope-like function [9]. As a result, the accelerations of loads across a bridge subjected to traffic loads were localized [8] for specific positions.

Traffic loading usually excites the structural modes that correspond to vehicle frequencies. The *Ontario Highway Bridge Design Code* [10] recommends increasing the amplification factor when the dominant natural frequencies of a structure range from 2 Hz to 5 Hz, and the American Association of State Highway and Transportation Officials (AASHTO) specifies that the frequency of general trucks should be 2.5 Hz [11]. Bartos [11] also suggested that the dynamic amplification effect could exceed limitations when the structural frequencies are between 1.5 Hz and 5 Hz. The vehicle-bridge interaction is also distorted by driving frequencies, which are dependent on the duration of a vehicle crossing a single stringer [12,13]. Brewick [14] discovered that these distortions of modal information increase the uncertainty of a damping estimation based on OMA schemes.

This study focuses on nonstationarity due to traffic loading, and its effect on OMA-based damping estimation. The effect of traffic loading was examined via the field-measured data from a

* Corresponding author.

E-mail address: hokyungk@snu.ac.kr (H.-K. Kim).

suspension bridge. A signal stationarization algorithm was proposed by introducing an amplitude-modulating (AM) function, and was applied to the operational monitoring data obtained from a suspension bridge for damping estimation.

2. Investigating the TIV of a suspension bridge

2.1. The Sorok Bridge

The Sorok Bridge (Fig. 1) is a self-anchored mono-cable suspension bridge in Korea connecting Sorok Island with the mainland. The bridge has a total length of 470 m, which consists of a 250 m main span and two symmetric side spans of 110 m. The total width of its steel box girders is 15.7 m, which provides two traffic lanes. The bridge was opened to traffic in March 2009. Since then, a series of dynamic tests have been carried out for detailed inspections and model updates for maintenance. Table 1 summarizes the modal frequencies of the bridge, as identified by OMA using frequency domain decomposition (FDD) of the data obtained from ambient vibration testing (AVT). Table 1 also includes the calculated natural frequencies obtained from the updated finite element model based on manual tuning and a parameterized sensitivity-based model updating approach [15,16]. The coincidences between the measured and calculated frequencies are shown in Table 1.

2.2. Data acquisition from AVT

Two accelerometers deployed at the center of the main span were utilized to measure the vertical acceleration of the deck with a sampling frequency of 100 Hz. The corresponding displacement of the deck was simultaneously measured using a laser displacement transducer equipped as a built-in sensor for the monitoring of the operational behavior of the bridge. Wind direction and wind velocity were recorded via an ultrasonic anemometer installed on the bridge deck. The available data were divided into 10 min intervals for an in-depth investigation.

Even though the field tests were basically planned to secure data from AVT, a heavy truck was also prepared to create the high-level excitation of an operating condition. A series of measured accelerations from the suspension bridge were analyzed to confirm the properties of the TIV. In particular, two types of testing—a truck-loading test and an ambient vibration test using normal vehicles—were considered in order to investigate the characteristics of TIV according to different types of vehicles. The truck-loading test was performed using a three-axle truck with a total mass of 25 t at speeds of 25 km·h⁻¹ and 40 km·h⁻¹. The bridge was not closed to normal traffic, but the latter would have been relatively minor in weight compared with the truck and would have been of little value in investigating truck-induced vibration.



Fig. 1. The Sorok Bridge.

Table 1
The modal frequencies of the Sorok Bridge.

Mode	AVT (Hz)	Calculated (Hz)
1st vertical	0.406	0.403
2nd vertical	0.478	0.463
3rd vertical	0.839	0.829
1st lateral	0.521	0.521
1st torsional	1.550	1.530

2.3. Nonstationary characteristics in TIV

To examine the nonstationary effect caused by traffic loading, a stationary response was utilized as a reference, which satisfied the assumptions of classic OMA. To select a stationary response from among the set of operational monitoring data, the kurtosis value was evaluated for a series of vibration data. The kurtosis value data were lower than 10 and contained no peak responses that could be classified as stationary [17]. In particular, the highest wind velocity was selected to represent the stationary data in order to secure a high signal-to-noise ratio.

The TIV data statistics are summarized in Table 2. In Table 2, the TIV data induced by the truck loading are referred to as “heavy truck,” while the vibrations measured during normal operations are classified as “ordinary vehicle.”

The stationary excitation data shown in Fig. 2 has no extreme peaks due to passing vehicles, and the kurtosis value was identified as 4.17, which indicates a stationary status. The power spectral density (PSD) shows that the main structural modes—the first (0.415 Hz) and third vertical modes (0.842 Hz)—were dominant.

In contrast, as shown in Fig. 3, the structural modes around 2 Hz were amplified when a heavy truck passed over the bridge. As a truck entered the main span, the amplitude increased gradually, and invoked a nonstationary response. The kurtosis value was 12.47, which exceeded the criterion for a stationary mode.

Ordinary vehicles also amplified a higher mode of structures compared with a stationary mode, as shown in Fig. 4. The structural modes of 4–5 Hz were excited by lighter vehicles that excited relatively higher frequencies. The kurtosis value was 49.69, which exceeded the stationary criterion of 10, and indicated a nonstationary mode.

Fig. 5 represents the time-frequency distribution calculated using a short-time Fourier transform. A Hamming window was used to calculate a spectrogram with segment lengths of 2¹³ and a 50% overlap. Fig. 5 clearly shows that the higher structural modes of 2–5 Hz were particularly excited when a vehicle crossed the bridge.

3. Signal stationarization using amplitude-modulating function

3.1. Amplitude-modulating function

Chiang and Lin [18] proposed a method for the identification of modal parameters from response data gathered from a structure

Table 2
Statistics of TIV and corresponding wind velocity.

	Vibration categorized as stationary	Vibration induced by heavy truck	Vibration induced by ordinary vehicle
Root-mean-square (Gal) ^a	0.49	2.61	1.74
Peak (Gal)	2.98	21.82	26.08
Kurtosis	4.17	12.47	49.69
10 min averaged wind velocity (m·s ⁻¹)	8.81	6.91	2.43

^a 1 Gal = 1 × 10⁻² m·s⁻².

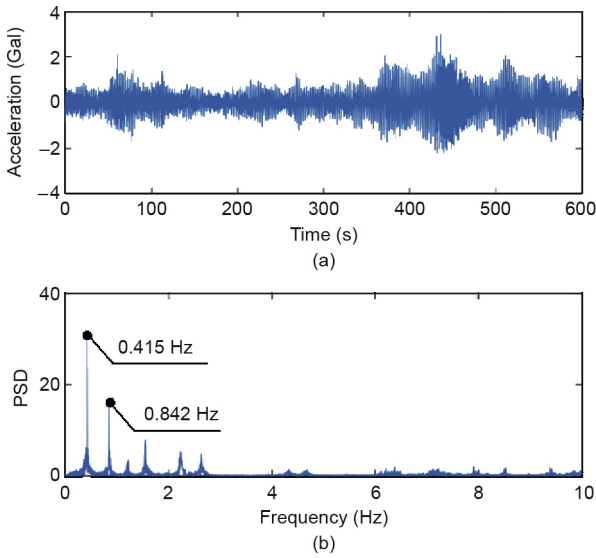


Fig. 2. (a) Measured acceleration and (b) PSD for stationary excitation.

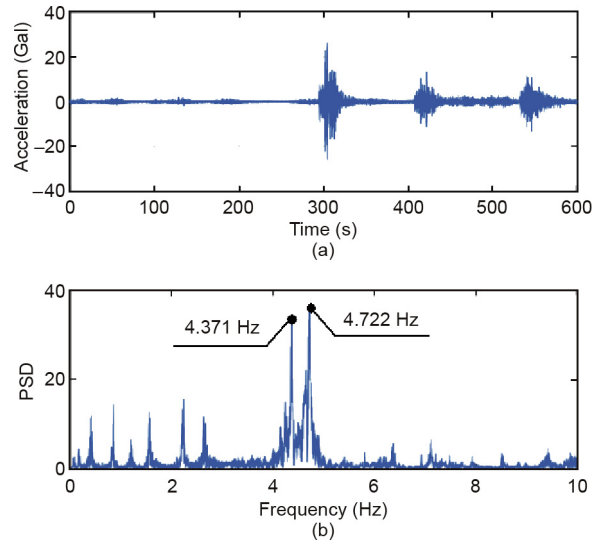


Fig. 4. (a) Measured acceleration and (b) PSD for an ordinary vehicle.

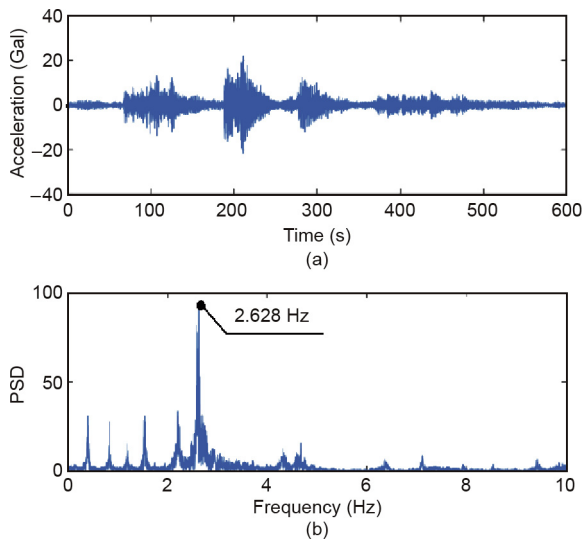


Fig. 3. (a) Measured acceleration and (b) PSD for a heavy truck.

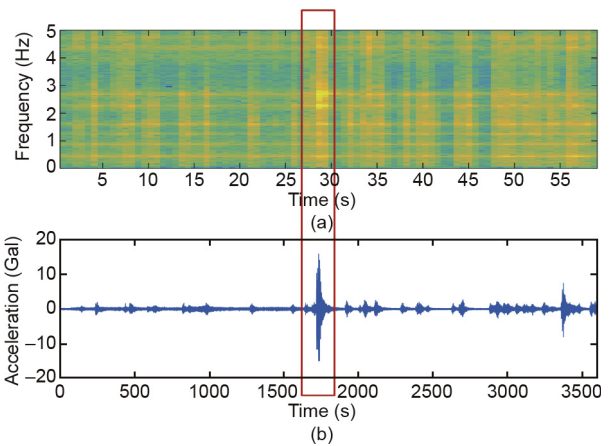


Fig. 5. (a) Time-frequency distribution and (b) corresponding measured acceleration (14 July 2012, 6:00 a.m.).

under nonstationary ambient vibration. As shown in Fig. 6, nonstationary measured acceleration $a(t)$ can be modeled as a product of stationary acceleration $\tilde{a}(t)$ and the AM function $\Gamma(t)$, as follows:

$$a(t) = \Gamma(t)\tilde{a}(t) \quad (1)$$

With this model, the stationary process can be approximated from the nonstationary response via modulation with the AM function $\Gamma(t)$. The AM function can be evaluated from the temporal root-mean-square (RMS) of nonstationary data [19] as follows:

$$\Gamma(t) = C\sqrt{\frac{1}{T_w} \int_{t-T_w/2}^{t+T_w/2} a^2(\tau)d\tau} \quad (2)$$

where C is the expectation of the square root for the ergodic process portion and T_w is the segment length for calculating the temporal RMS. As a result, the approximate stationary acceleration can be obtained as follows:

$$\tilde{a}(t) = a(t)/\Gamma(t) \quad (3)$$

3.2. Application of AM to operational monitoring data

The proposed stationarization process was applied to the operational monitoring data obtained from the Sorok Bridge. The AM function was evaluated by calculating the temporal RMS function of the measured acceleration. The approximate stationary acceleration was then extracted by dividing the measured acceleration by the AM function.

Fig. 7(a) and Fig. 7(b) show the traffic-induced accelerations before and after signal stationarization, respectively. Before the signal stationarization process, the measured acceleration in the time history was localized. The kurtosis value exceeded the criteria of 10. However, after the stationarization process, the peaks due to traffic loading were removed from the time history. The kurtosis value also decreased from 12.83 to 2.36.

Fig. 8 compares the normalized PSDs before and after signal stationarization. The frequency components around vehicle frequencies of 2–5 Hz were clearly reduced with an application of the AM function during the signal stationarization. As a result, the PSD of the stationarized data showed a frequency component that was similar to the PSD of the stationary case.

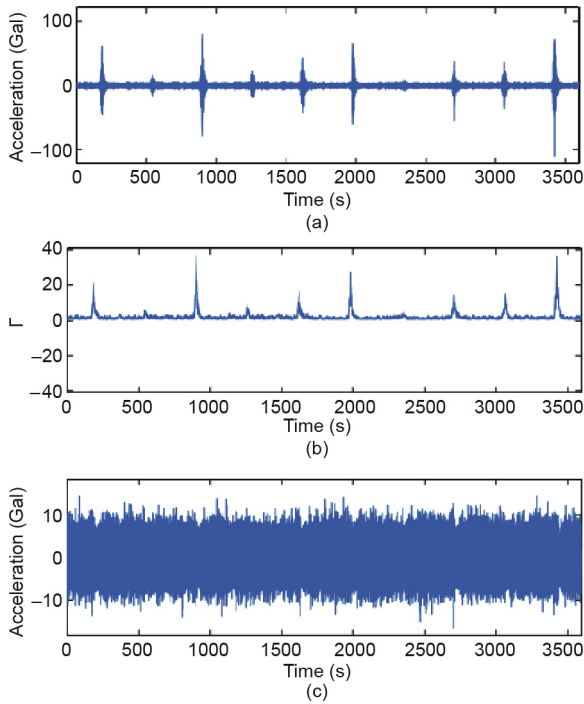


Fig. 6. A nonstationary process modeling with AM function. (a) Measured acceleration $a(t)$; (b) AM function $\Gamma(t)$; (c) stationary acceleration $\bar{a}(t)$.

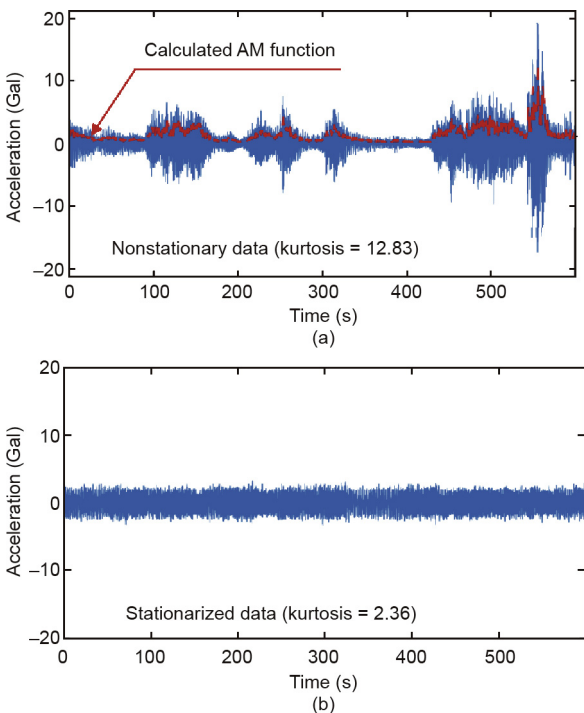


Fig. 7. Measured acceleration (a) before and (b) after signal stationarization with the AM function.

4. OMA-based damping estimation with signal stationarization

4.1. Parameter selection for OMA-based damping estimation

A natural excitation technique (NExT)-eigensystem realization algorithm (ERA) was applied to the one-hour acceleration data that

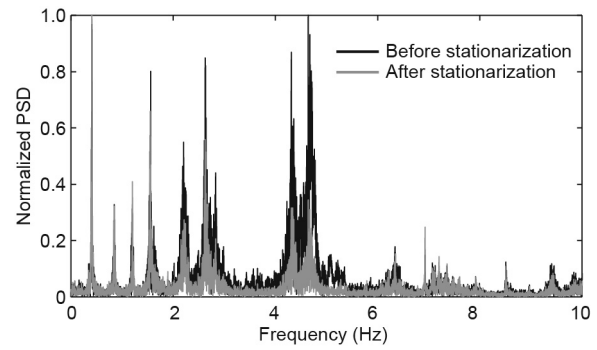


Fig. 8. Normalized PSD of measured acceleration before and after signal stationarization with the AM function.

were recorded for four days, from 13 June to 16 June 2016. To calculate the auto correlation function of the measured acceleration in the NExT procedure, a Hanning window with a length of 2^{15} was applied with an overlap of 50% [2]. With this parameter setup, the frequency resolution was 0.0031 Hz for an average number of 21. Fig. 9 shows a calculated correlation function simulating the impulse response function (IRF) of the structure.

The size of the Hankel matrix was selected based on the shape of the calculated IRF, as shown in Fig. 9. For example, the time required for a calculated IRF to decrease to a level of 50% was identified from the positive/negative envelope function of IRF ($t_1 = 17.77$ s, $t_2 = 18.08$ s). The longer version (18.08 s) was then selected.

OMA-based damping estimation is sensitive to the system order of the ERA. To obtain a converged damping ratio, a system order should be selected with the help of a stabilization diagram, as shown in Fig. 10. A series of modal analyses should be performed to examine all system orders from 1 to 50, and to identify and record the first vertical mode (0.406 Hz) that satisfies criteria such as frequency range, positive damping, and extended modal amplitude coherence (EMAC). Next, the median value of the identified damping ratios should be determined.

For the selection of an appropriate segment length for signal stationarization, a parametric study was carried out for the one-day operational monitoring data obtained from the Sorok Bridge. Fig. 11 shows the mean and coefficient of variance (COV) of the estimated damping ratio according to the segment ratio, which is defined as the ratio between the segment length and the target natural period (T_n). As shown in Fig. 11, the mean values of the estimated damping ratios converged to 1% from the segment ratio

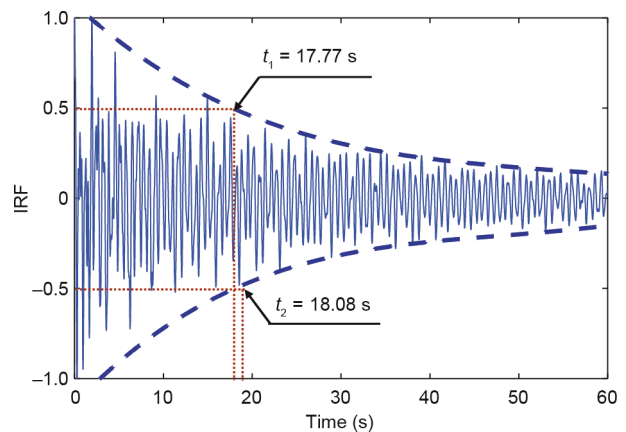


Fig. 9. Determining a utilized time length of IRF based on envelope function.

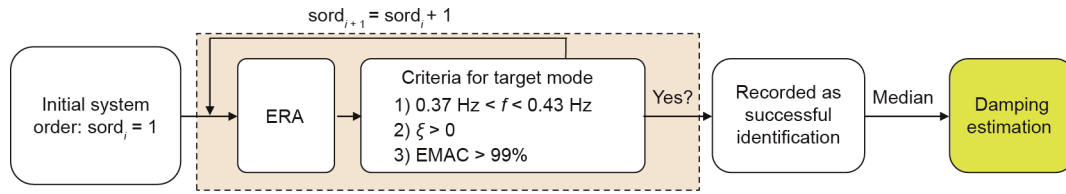


Fig. 10. Procedure for selecting a system order and identifying the damping ratio.

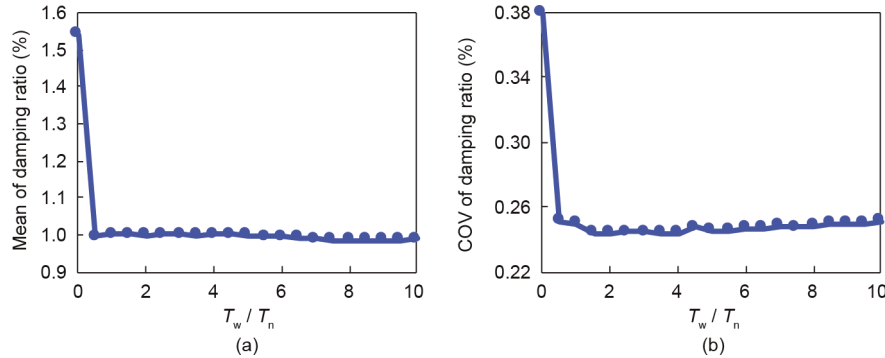


Fig. 11. Statistics of the estimated damping ratio for the Sorok Bridge according to the segment ratio. (a) Mean of the estimated damping ratio; (b) COV of the estimated damping ratio.

of 0.5, while the COV value became stable from the segment ratio of 1.5. Therefore, a segmental length that is 1.5 times larger than the target natural period seems to be recommendable for the signal stationarization process using moving RMS for the Sorok Bridge.

4.2. Estimated damping ratio with signal stationarization

Three comparative approaches were implemented in estimating the damping ratio of the first mode of the Sorok Bridge. The first case did not consider stationarization and simply applied NEXTERA to the measured data; hereafter, this case is referred to as “without stationarization (w/o stationarization).” An identified damping ratio with signal stationarization is hereafter referred to as “w/ stationarization,” and “combined” indicates that a signal stationarization was selectively applied depending on the kurtosis value of the measured acceleration. As Guo [17] suggested, a kurtosis value of 10 was utilized as a criterion to differentiate

stationary from nonstationary measured data. If the kurtosis value of the measured acceleration was larger than 10, a signal stationarization procedure was applied. Eighty cases of measured accelerations were identified as nonstationary data from among 96 datasets. A segment length of five times the target natural period was applied for signal stationarization, as shown in Fig. 11.

Fig. 12 shows the estimated damping ratio of the Sorok Bridge during operation. The estimated damping ratios fluctuated according to time slots that extended from morning until night. The damping ratios appeared to be dependent on the volume of traffic. The severe scatterings noted on July 14 and 15 were reduced when a signal stationarization process was applied.

The mean value and standard deviation of the damping ratio for the first vertical mode decreased after signal stationarization. The COVs of the estimated damping ratios after signal stationarization were 34%, which were acceptable when compared with previous AVT practices [20–24].

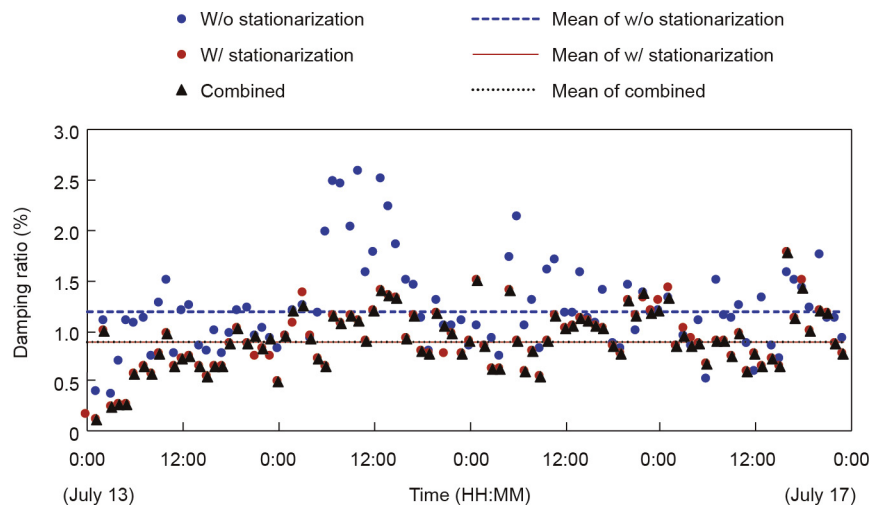


Fig. 12. Estimated modal damping ratio of the Sorok Bridge according to signal stationarization.

5. Conclusions

This study focused on nonstationarity due to traffic loading on the Sorok Bridge in Korea, and its effect on OMA-based damping estimation. A literature survey and field-monitoring data confirmed that TIV was localized, resulting in a nonstationary response. The structural modes of vehicle frequencies that ranged from 2 Hz to 5 Hz were amplified by traffic loading, but lower structural modes were dominated by stationary excitation. A signal stationarization process that adopted an AM function was proposed. The AM function was obtained from envelope-type output-only data induced by running vehicles, and was applied to modulate nonstationary components. Values for the nonstationary effect and frequency distortion due to vehicles were successfully reduced by a signal stationarization procedure. After signal stationarization, the kurtosis value was significantly decreased and the PSD function approximated that of the stationary data. As a result, the over/underestimated damping ratio due to TIV was recovered and the uncertainty of the estimated damping ratios was reduced by applying the signal stationarization process. Even though this study only considered the AM function for stationarization, alternative approaches such as the Hilbert transform can be extensively examined in further study.

Acknowledgements

This work was supported by the National Research Foundation of Korea (NRF) grant funded by the Korean government (MSIP) (2017R1A2B4008973) and also supported by grants (17SCIPB119960-02) from the Ministry of Land, Infrastructure and Transport of the Korean Government. This work was also partially supported by the BK21 PLUS research program of the National Research Foundation of Korea and the New Technology Research Center for Bridges through the Institute of Engineering Research at Seoul National University. The authors are also grateful to the owner of the Sorok Bridge, TM E&C, and to the Korea Infrastructure Safety and Technology Corporation (KISTEC) for sharing operational monitoring data.

Compliance with ethics guidelines

Sunjoong Kim and Ho-Kyung Kim declare that they have no conflict of interest or financial conflicts to disclose.

References

- [1] Kim SJ, Kim HK, Calmer R, Park J, Kim GS, Lee DK. Operational field monitoring of interactive vortex-induced vibrations between two parallel cable-stayed bridges. *J Wind Eng Ind Aerodyn* 2013;123(Pt A):143–54.
- [2] Kim S, Park J, Kim HK. Damping identification and serviceability assessment of a cable-stayed bridge based on operational monitoring data. *J Bridge Eng* 2016;22(3):04016123.
- [3] Feng MQ, Fukuda Y, Chen YB, Soyoz S, Lee S. Long-term structural performance monitoring of bridges: Phase II: Development of baseline model and methodology for health monitoring and damage assessment. Final report. Sacramento: California Department of Transportation; 2006. Oct. Report No.: CA07-0245. Contract No.: RTA59A0311.
- [4] Guo YL, Kareem A, Ni YQ, Liao WY. Performance evaluation of Canton Tower under winds based on full-scale data. *J Wind Eng Ind Aerodyn* 2012;104–106:116–28.
- [5] Lin CS, Chiang DY. Modal identification from nonstationary ambient response data using extended random decrement algorithm. *Comput Struct* 2013;119:104–14.
- [6] Kim CW, Kawatani M, Kim KB. Three-dimensional dynamic analysis for bridge–vehicle interaction with roadway roughness. *Comput Struct* 2005;83(19–20):1627–45.
- [7] Kim CW, Kawatani M. Pseudo-static approach for damage identification of bridges based on coupling vibration with a moving vehicle. *Struct Infrastruct Eng* 2008;4(5):371–9.
- [8] Guo WH, Xu YL. Fully computerized approach to study cable-stayed bridge–vehicle interaction. *J Sound Vib* 2001;248(4):745–61.
- [9] Sun H, Feng DM, Liu Y, Feng MQ. Statistical regularization for identification of structural parameters and external loadings using state space models. *Comput-Aided Civ Infrastruct Eng* 2015;30(11):843–58.
- [10] Ontario Ministry of Transportation, Quality and Standards Division. Ontario highway bridge design code. 3rd ed. Ontario: Ontario Ministry of Transportation, Quality and Standards Division; 1991.
- [11] Bartos MJ. Ontario writes new bridge code. *Civil Eng—ASCE* 1979;49(3):56–61.
- [12] Lin CW, Yang YB. Use of a passing vehicle to scan the fundamental bridge frequencies: An experimental verification. *Eng Struct* 2005;27(13):1865–78.
- [13] Majka M, Hartnett M. Effects of speed, load and damping on the dynamic response of railway bridges and vehicles. *Comput Struct* 2008;86(6):556–72.
- [14] Brewick PT. Improving the quantification and estimation of damping for bridges under traffic loading [dissertation]. New York: Columbia University; 2014.
- [15] Park W, Kim HK, Jongchil P. Finite element model updating for a cable-stayed bridge using manual tuning and sensitivity-based optimization. *Struct Eng Int* 2012;22(1):14–9.
- [16] Park W, Park JY, Kim HK. Candidate model construction of a cable-stayed bridge using parameterised sensitivity-based finite element model updating. *Struct Infrastruct Eng* 2015;11(9):1163–77.
- [17] Guo YL. Nonstationary system identification techniques [dissertation]. Notre Dame: University of Notre Dame; 2015.
- [18] Chiang DY, Lin CS. Identification of modal parameters from nonstationary ambient vibration data using correlation technique. *AIAA J* 2008;46(11):2752–9.
- [19] Newland DE. An introduction to random vibrations, spectral & wavelet analysis. 3rd ed. Mineola: Dover Publications, Inc.; 2012.
- [20] Benedettini F, Gentile C. Operational modal testing and FE model tuning of a cable-stayed bridge. *Eng Struct* 2011;33(6):2063–73.
- [21] Brownjohn JMW, Magalhães F, Caetano E, Cunha Á. Ambient vibration re-testing and operational modal analysis of the Humber Bridge. *Eng Struct* 2010;32(8):2003–18.
- [22] Magalhães F, Cunha Á, Caetano E, Brincker R. Damping estimation using free decays and ambient vibration tests. *Mech Syst Sig Process* 2010;24(5):1274–90.
- [23] Magalhães F, Caetano E, Cunha Á, Flamand O, Grillaud G. Ambient and free vibration tests of the Millau Viaduct: Evaluation of alternative processing strategies. *Eng Struct* 2012;45:372–84.
- [24] Reynders E, Houbrechts J, De Roeck G. Fully automated (operational) modal analysis. *Mech Syst Sig Process* 2012;29:228–50.